Sponge Prokaryote Communities in Taiwanese Coral Reef and Shallow Hydrothermal Vent Ecosystems

F. J. R. C. Coelho, D. F. R. Cleary, N. C. M. Gomes, A. R. M. Pólonia, Y. M. Huang, L.-L. Liu & N. J. de Voogd

Microbial Ecology

ISSN 0095-3628
Volume 75
Number 1

Microb Ecol (2018) 75:239-254
DOI 10.1007/s00248-017-1023-x

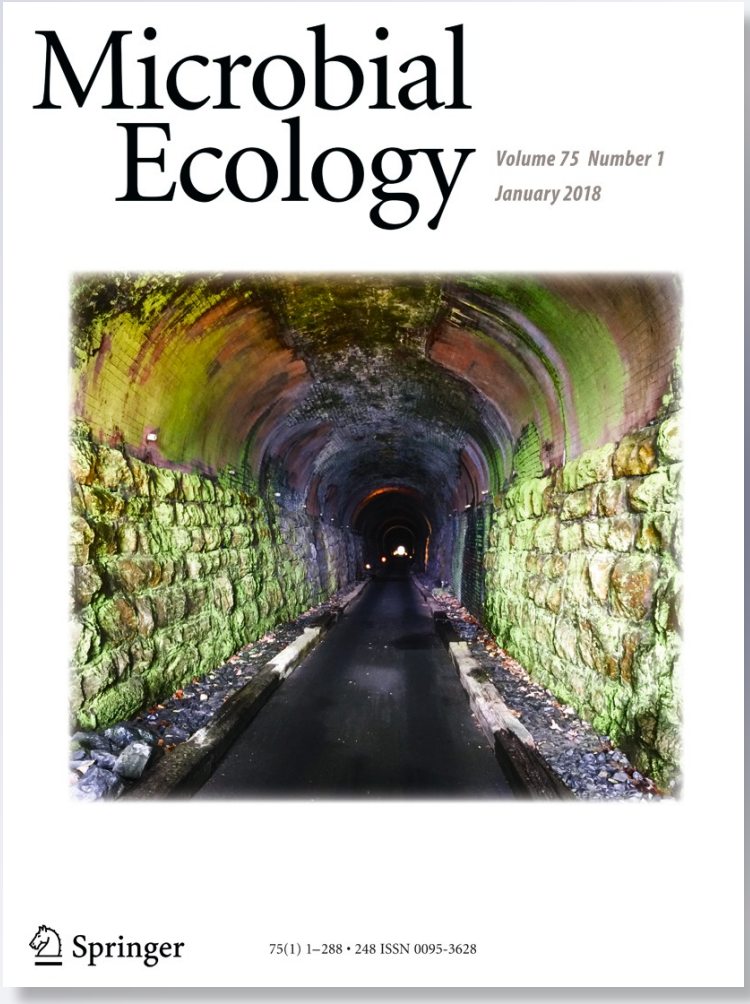

Springer

Microb Ecol (2018) 75:239–254
DOI 10.1007/s00248-017-1023-x

INVERTEBRATE MICROBIOLOGY

Sponge Prokaryote Communities in Taiwanese Coral Reef and Shallow Hydrothermal Vent Ecosystems

F. J. R. C. Coelho[1] · D. F. R. Cleary[1] · N. C. M. Gomes[1] · A. R. M. Pólonia[1,2] · Y. M. Huang[3,4] · L.-L. Liu[5] · N. J. de Voogd[4]

Received: 12 April 2017 / Accepted: 15 June 2017 / Published online: 11 July 2017

Abstract Previously, it was believed that the prokaryote communities of typical 'low-microbial abundance' (LMA) or 'non-symbiont harboring' sponges were merely subsets of the prokaryote plankton community. Recent research has, however, shown that these sponges are dominated by particular clades of Proteobacteria or Cyanobacteria. Here, we expand on this research and assess the composition and putative functional profiles of prokaryotic communities from LMA sponges collected in two ecosystems (coral reef and hydrothermal vent) from vicinal islands of Taiwan with distinct physicochemical conditions. Six sponge species identified as *Acanthella cavernosa* (Bubarida), *Echinodictyum asperum*, *Ptilocaulis spiculifer* (Axinellida), *Jaspis splendens* (Tetractinellida), *Stylissa carteri* (Scopalinida) and *Suberites* sp. (Suberitida) were sampled in coral reefs in the Penghu archipelago. One sponge species provisionally identified as *Hymeniacidon* novo spec. (Suberitida) was sampled in hydrothermal vent habitat. Each sponge was dominated by a limited set of operational taxonomic units which were similar to sequences from organisms previously obtained from other LMA sponges. There was a distinct bacterial community between sponges collected in coral reef and in hydrothermal vents. The putative functional profile revealed that the prokaryote community from sponges collected in hydrothermal vents was significantly enriched for pathways related to DNA replication and repair.

Keywords Archaea · Bacteria · Low microbial abundance sponges · Hydrothermal vent · Reef coral

Introduction

Microbial symbionts play key roles in the functioning and survival of eukaryotic organisms [1, 2]. Sponge-microbe associations represent a model of host-microbe interaction that has been the focus of extensive research [3]. The sponge microbiome has been shown to have a profound impact on sponge health, ecology and evolution [4]. For example, although the main means of carbon acquisition is heterotrophic (filter feeding), sponges can sometimes obtain more than 50% of their energy requirements from their photosymbionts [5]. The functional potential of sponge-enriched microorganisms further indicates that they support, at least in part, other metabolic processes such as ammonium and nitrite oxidation, nitrogen fixation and sulfate reduction [4]. The interest in these associations has been, furthermore, fostered by the sponge's ability to produce biologically active secondary metabolites, which, in some cases, have been directly linked to sponge-enriched microbial symbionts [6, 7]. Microbial abundance, composition, diversity and specificity can vary greatly among sponge species including species in the same habitat [8–11].

Electronic supplementary material The online version of this article (doi:10.1007/s00248-017-1023-x) contains supplementary material, which is available to authorized users.

✉ N. J. de Voogd
nicole.devoogd@naturalis.nl

[1] Department of Biology & CESAM, University of Aveiro, Campus de Santiago, 3810-193 Aveiro, Portugal

[2] Present address: Center for Neuroscience and Cell Biology, University of Coimbra, 3004-504 Coimbra, Portugal

[3] Department of Marine Recreation, National Penghu University of Science and Technology, Penghu, Taiwan

[4] Naturalis Biodiversity Center, Leiden, the Netherlands

[5] Department of Oceanography, National Sun Yet-Sen University, Kaohsiung, Taiwan

Sponge species harbouring very high densities of microorganisms (10^9 cells per gram wet weight of sponge) have been previously designated as HMA (high microbial abundance) sponges, while sponge species harbouring lower numbers of such symbionts (10^5 to 10^6 cells per gram wet weight of sponge) have been designated as LMA (low microbial abundance) sponges [12]. In addition to housing numbers of microorganisms similar to those found in seawater, LMA sponges have been shown to have lower microbial diversity (mainly consisting of taxa assigned to Proteobacteria, Cyanobacteria and Archaea), higher pumping rates, wider aquiferous canals and larger choanocyte chambers when compared to HMA sponges [13]. Hochmuth et al. (2010) also suggested that the absence of the candidate phylum Poribacteria and supA type polyketide synthase genes in LMA sponges endows them with a distinct fatty acid profile (in particular the lack of methyl-branched fatty acids).

The microbiome composition of LMA sponges and its stability in different habitats is still far from being completely understood. The majority of studies have either concentrated on HMA sponges or did not clearly distinguish between HMA and LMA sponges [14]. There is also a lack of knowledge regarding the extent of species-specific microbial symbionts in LMA sponges and their stability under changing environmental conditions. In the present study, we investigated and compared the prokaryote communities of LMA sponges located in highly contrasting ecosystems, (coral reefs and low pH vent) in Taiwanese waters.

Taiwan is located on the northern border of the 'Coral Triangle', recognized as a global centre of marine biodiversity and a global priority for conservation, which includes the Philippines, Malaysia and Indonesia [15, 16]. With the exception of the western sandy coastline of the Taiwanese mainland, coral reefs can be found along the northern, eastern and southern rocky coasts and offshore islands including the Penghu Islands and Kueishan Islet. Much of these reefs have been degraded by human activity, but thriving reefs with high coral cover can still be found in certain locations including the isolated southern Penghu Islands [17]. Coral reefs of the Penghu Islands also harbor a diverse sponge community with over 60 species recorded in shallow-water reef habitat [18, 19]. Along the southern coast of the main island, Magong, populations of the giant barrel sponge, *Xestospongia testudinaria* and other species, such as *Cinachyrella* spp., adapted to elevated levels of sedimentation can be found, while the southern offshore islands harbour dominant populations of *Agelas nemoechinata* Hoshino, 1985, *Aaptos suberitoides* Bronsted, 1934, and *Acanthella cavernosa* Thiele, 1903 [19].

The shallow-water hydrothermal vent system off the Kueishan Islet ('Turtle Mountain'), NE Taiwan, was first documented in 1999 [20]. The hydrothermal vents are located at a depth of 8 to 20 m and are characterized by acidic (pH = 1.52–6.96) and sulfur-rich discharges that can reach temperatures of 45–115 °C. The waters near the hydrothermal vents are poor in nutrients but rich in trace elements such as Fe, Cu, Al and Mn [21]. In this extreme physical environment, benthic extremophiles include microorganisms [22–24], crustaceans [24], unknown sea anemones, algae (Rhodophyta and Chlorophyta), polycheates and sponges (pers. obs. YM Huang). In this study, our goal was to investigate the richness, composition and putative function of prokaryote communities in LMA sponge species located in Taiwanese coral reef and shallow hydrothermal vent ecosystems.

Materials and Methods

Location

The Penghu archipelago (Fig. 1), off the western coast of Taiwan in the Taiwan Strait, consists of approximately 90 islands and islets. The islands mainly consist of oceanic basalt rock that resulted from the discharge of magma from submarine volcanic crevasses 8–16 million years ago [25]. Typical fringing reefs dominate most of the coastal areas. The hydrology around the islands is significantly influenced by the cold, southbound Chinese Coastal Current, the warm northbound South China Sea Current and in part by the Kuroshio Current. The anfractuous coastline of the islands, convergence of three main currents, diurnal alternation of tidal current and upwelling result in a complex hydrological condition. Annual variation of mean sea surface temperature ranges from 21 to 28 °C; however, extremely cold seawater temperature (ca. 11 °C) can strike the islands caused by the Chinese Coastal Current every few decades [26]. In addition to this, the abundance and biodiversity of subtidal sponges in the coral reef system has been estimated to be high.

Kueishan Islet (121°57′ E, 24°50′ N; Fig. 1), approximately 10 km off the coastline of the Yilan County, NE Taiwan, is at the tectonic junction of the fault system extension of Taiwan and the southern rifting end of the Okinawa Trough [27]. As the youngest in the region, the island formed during the last eruption that occurred ca. 7000 years ago. There are more than 30 hydrothermal vents over an area of ~0.5 km^2 east of the islet at a depth of <30 m, emitting hydrothermal fluids and volcanic gases [21]. Yellow vents discharging elemental sulfur particles have recorded temperatures of 78–116 °C (mean 106 ± 9 °C) and pH values of 1.52–6.32 (mean 2.49 ± 0.72), while vents discharging whitish fluids have lower temperatures of 30–65 °C (mean 51 ± 8 °C) and pH values of 1.84–6.96 (mean 3.20 ± 1.17). In the hydrothermal site, all sponge specimens were collected within a 5-m range of white vents (121°57.690′ E, 24°50.053′ N); no sponges were observed at yellow vents. Only two sponge species were found at the white vents, both belonging to the genus *Hymeniacidon* (order: Suberitida). Both species are considered new to science.

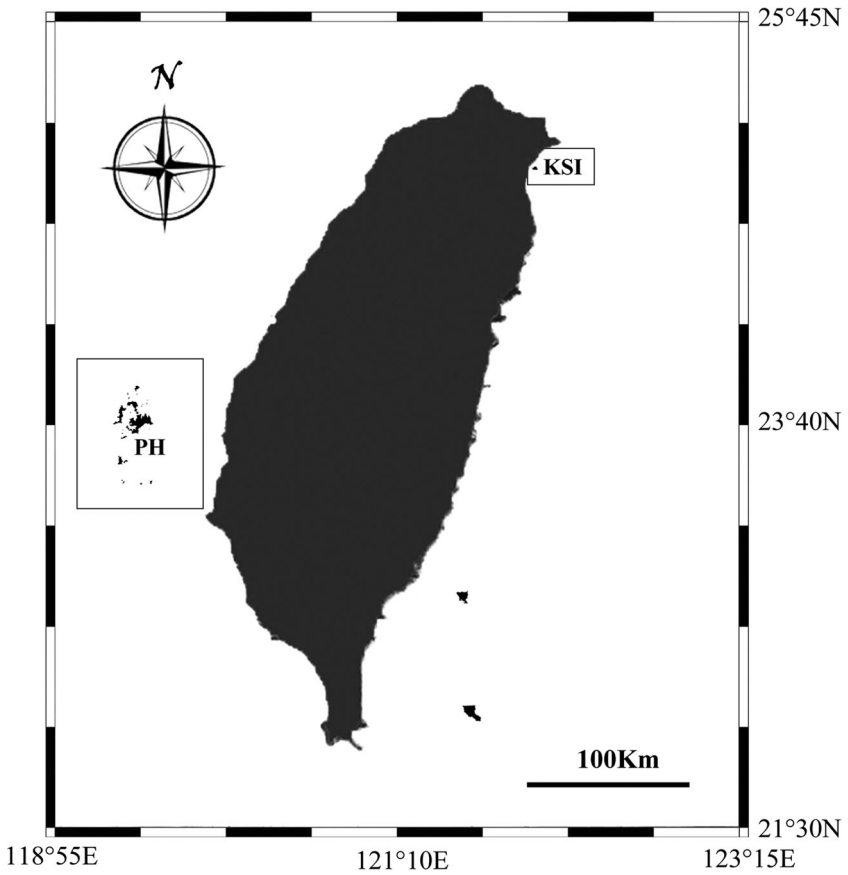

Fig. 1 Sampling locations of LMA sponges. Coral reef (Penghu Island; *PH*) and low pH shallow hydrothermal vent (Kueishan Islet; *KSI*) of Taiwan

Sampling Site

In the present study, we sampled six shallow water LMA sponge species in coral reef habitat in the Penghu Islands and one sponge species at the shallow water hydrothermal vent off Kueishan Island islet. The six coral reef sponge species were identified by NJ de Voogd as *A. cavernosa* (order: Bubarida), *Echinodictyum asperum*, *Ptilocaulis spiculifer* (order: Axinellida), *Jaspis splendens* (order: Tetractinellida), *Stylissa carteri* (order: Scopalinida) and *Suberites* aff. *diversicolor* (order: Suberitida) and were sampled in reefs of the Penghu archipelago. One sponge species provisionally identified as *Hymeniacidon* novo spec. was sampled in hydrothermal vent habitat. Two to four replicates were sampled per species. Sponges were photographed in situ, collected using scuba diving, brought back to the laboratory and preserved in 95% ethanol for further identification and molecular work. Three seawater samples were collected from coral reef habitat by filtering 1 l of seawater (collected at 1 m depth) through a Millipore® White Isopore Membrane Filter (GTTP04700, 47-mm diameter, 0.22-μm pore size). All sponge specimens have been deposited at Naturalis Biodiversity Center.

DNA Extraction and Sequencing

PCR-ready total community DNA (TC-DNA) was isolated from sponge and seawater samples using the FastDNA® SPIN Kit (MP Biomedicals) following the manufacturer's instructions. The membrane filter (seawater) or sponge samples were each cut into small pieces and transferred to Lysing Matrix E tubes containing a mixture of ceramic and silica particles. The microbial cell lysis was performed in the FastPrep® Instrument (Q Biogene) for 80 s at speed 6.0. Extracted DNA was eluted into DNase/pyrogen-free water to a final volume of 50 μl and stored at −20 °C until use. The 16S rRNA gene V3V4 variable region PCR primers 341F 5′-CCTACGGGNGGCWGCAG-3′ and 785R 3′-GACTACHVGGGTATCTAATCC-5′ with barcode on the forward primer were used in a 28 cycle PCR assay using the HotStarTaq Plus Master Mix Kit (Qiagen, USA) under the following conditions: 94 °C for 3 min, followed by 28 cycles of 94 °C for 30 s, 53 °C for 40 s and 72 °C for 1 min, after which a final elongation step at 72 °C for 5 min was performed. After amplification, PCR products were checked in 2% agarose gel to determine the success of amplification and

the relative intensity of bands. Multiple samples were pooled together in equal proportions based on their molecular weight and DNA concentrations. Pooled samples were purified using calibrated Ampure XP beads. Pooled and purified PCR product was used to prepare the DNA library following the Illumina TruSeq DNA library preparation protocol. Next-generation, paired-end sequencing was performed at MRDNA (Molecular Research LP; http://www.mrdnalab.com/; last checked 18 November 2016) on an Illumina MiSeq device (Illumina Inc., San Diego, CA, USA) following the manufacturer's guidelines. Sequences from each end were joined following Q25 quality trimming of the ends followed by reorienting any 3′–5′ reads back into 5′–3′ and removal of short reads (<150 bp). The resultant files were analysed using the QIIME (Quantitative Insights Into Microbial Ecology; [28] software package (http://www.qiime.org/; last checked 20 January 2017).

16S rRNA Gene Sequencing Analysis

In QIIME, fasta and qual files were used as input for the split_libraries.py script. Default arguments were used except for the minimum sequence length, which was set at 250 bps after removal of forward primers and barcodes. In addition to user-defined cut-offs, the split_libraries.py script performs several quality filtering steps (http://qiime.org/scripts/split_libraries.html). Operational taxonomic units (OTUs) were selected using UPARSE with usearch7 [29]. The UPARSE sequence analysis tool provides clustering, chimera checking and quality filtering on de-multiplexed sequences. Chimera checking was performed using the UCHIME algorithm [30]. The quality filtering as implemented in usearch7 filters noisy reads, and preliminary studies suggest it gives results comparable to other denoisers such as AmpliconNoise but is much less computationally expensive (http://drive5.com/usearch/features.html; last checked 20 January 2017). First, reads were filtered with the -fastq_filter command and the following arguments -fastq_trunclen 250 -fastq_maxee 0.5 -fastq_truncqual 15. Sequences were then dereplicated and sorted using the -derep_fulllength and -sortbysize commands. OTU clustering was performed using the -cluster_otus command. An additional chimera check was subsequently applied using the -uchime_ref command with the gold.fa database (http://drive5.com/uchime/gold.fa). AWK scripts were then used to convert the OTU files to QIIME format. In QIIME, representative sequences were selected using the pick_rep_set.py script in QIIME using the 'most_abundant' method. Taxonomy was assigned to reference sequences of OTUs using default arguments in the assign_taxonomy.py script in QIIME with the rdp method [31]. In the assign_taxonomy.py function, we used a fasta file containing reference sequences from the Greengenes 13_8 release and the rdp classifier method. We used a modified version of the taxonomy file supplied with the Greengenes 13_8 release to map sequences to the assigned taxonomy. Finally, we used the make_otu_table.py script in QIIME to generate a square matrix of OTUs x SAMPLES. This was subsequently used as input for further analyses using the *R* package [32]. Sequence identifiers of closely related taxa of selected OTUs (≥1500 sequences) were downloaded using the NCBI Basic Local Alignment Search Tool (BLAST) command line 'blastn' tool with the -db argument set to nt [33]. Further details can be found in supportive information. The DNA sequences generated in this study can be downloaded from the NCBI SRA: SRP109605.

Statistical Analysis of 16S rRNA Gene Sequencing Data

A table containing the presence and abundance of all OTUs per sample was imported into *R* (https://www.r-project.org) using the read.csv() function. This table was used to compare community composition, estimate richness and assess the relative abundance of selected higher taxa. For the OTU table, singletons and OTUs not classified as bacteria or classified as chloroplasts and mitochondria were removed prior to statistical analysis.

We used a self-written function in *R* to estimate total rarefied OTU richness [34]. The OTU abundance matrix was $\log_e(x + 1)$ transformed (to normalize the distribution of the data), and a distance matrix was constructed using the Bray–Curtis index with the vegdist() function in the VEGAN package [35] in *R*. Variation in OTU composition was assessed with Principal Coordinates Analysis (PCO) using the cmdscale() function in *R* with the Bray–Curtis distance matrix as input. Variation among host species was tested for significance using the adonis() function in vegan. In the adonis analysis, the Bray–Curtis distance matrix of species composition was the response variable with biotope as independent variable. The number of permutations was set at 999; all other arguments used the default values set in the function. Weighted average scores were computed for OTUs on the first four PCO axes using the wascores() function in the vegan package. We tested for significant differences in the relative abundance of selected classes among host species with an analysis of deviance using the glm() function in *R*. Because the data was proportional, we first applied a glm with the family argument set to binomial. The ratio, however, of residual deviance to residual d.f. in the models substantially exceeded 1 so we set family to 'quasibinomial'. In the 'quasibinomial' family, the dispersion parameter is not fixed at one so that it can model over-dispersion. Using the glm model, we tested for significant variation among biotopes using the anova() function in *R* with the *F* test, which is most appropriate when dispersion is estimated by moments as is the case with quasibinomial fits. Detailed descriptions of the functions used here can be found in *R* (e.g., ?cmdscale) and online in reference manuals (http://cran.r-

project.org/web/packages/vegan/index.html). A heatmap was constructed to visualize the distribution of the dominant OTUs (≥1500 sequences). The heatmap was generated using the function heatmap2() in the *R* package gplots (http://www.cran.r-project.org/).

We constructed a phylogenetic tree that included the most abundant alphaproteobacterial OTUs (>1500 sequences), their closest related taxa based on the best BLAST hits, sequences assigned to Kiloniellales retrieved from Cleary et al. [8] (SRA049887) and sequences assigned to Alphaproteobacteria retrieved from Weigel and Erwin [40] (accession numbers: KT880397, KT880320, KT880309, KT880397, KT880329, KT880358, KT880292, KT880420, KT880289, KT880233, KT880453). Evolutionary distances were computed using the maximum composite likelihood method with a gamma distribution (four categories) and 500 bootstraps [36] using MEGA software (version 6.06) [37].

Predictive Gene Enrichment

To predict the metagenome of each sample, we used PICRUSt (http://picrust.github.com/picrust/—Version 1.0) [38]. PICRUSt is a bioinformatic tool that uses marker genes, in this case 16S rRNA, to predict metagenome gene functional content. A detailed description of these methods has been previously published [38, 39]. Briefly, the 'pick_closed_reference_otus.py' was used to pick OTUs against a reference collection with OTUs assigned at a 97% similarity. OTUs were selected using the GreenGenes release version 13_5 (http://greengenes.lbl.gov). The OTU table obtained was then normalized dividing each OTU by the known/predicted 16S copy number with 'normalize_by_copy_number.py' function. The 'predict_metagenomes.py' function was used to create a square matrix, containing normalized OTU abundance multiplied by each predicted functional trait abundance per sample. Output of the predict_metagenomes.py script consists of a table of gene (or functional) counts assigned to KEGG orthologs (KOs). Finally, the 'categorize_by_function.py' function was used to generate a square matrix with KEGG hierarchy collapsed at levels 2 and 3. We additionally used the '-a' option to calculate the Nearest Sequenced Taxon Index (NSTI). The script used is provided in the supporting information. We focused only on sponges that had at least three replicates and water samples. A table containing the presence and abundance of all KOs per sample was imported into *R* using the read.csv() function. This table was used to compare KO composition using the PCO and the adonis() function as described above. The square matrix containing the KEGG hierarchy collapse at levels 2 and 3 was used to compare the relative abundance of KOs assigned with specific pathways. We further tested for significant differences among host species with an analysis of deviance using the glm() function in *R*.

Results

Community Richness and Composition

The sequencing effort generated 418,669 sequences that were binned into to 6438 OTUs after quality screening and excluding OTUs assigned to chloroplasts and mitochondria. OTUs were assigned to 45 phyla, 117 classes and 165 orders. Prokaryote rarefied richness was highest in an *E. asperum* sample, followed by water, *J. splendens* and *P. spiculifer* samples (Fig. 2). *Suberites* sp. and *Hymeniacidon* sp. had the lowest estimated richness. In the PCO analysis, the first axis separated samples of *Hymeniacidon* sp. and one replicate of *Suberites* sp. from the rest of the samples (Fig. 3a). The second axis separated samples of *A. cavernosa* and *S. carteri* from the remaining samples (Fig. 3a). The third axis separated samples of *Suberites* sp. from the samples of *Hymeniacidon* sp. (Fig. 4a). The fourth axis separated samples of *J. splendens* from water samples (Fig. 4a). The biotope (sponge species or water) proved to be a significant determinant of prokaryote composition (adonis, $F_{7,22} = 3.09$, $R^2 = 0.590$, $P < 0.001$) and explained 59% of the variation in composition. Samples of *Hymeniacidon* sp. were characterized by the presence of a number of highly abundant OTUs assigned to the alphaproteobacterial class (Figs. 3b). *Hymeniacidon* sp. and *Suberites* sp. both hosted alphaproteobacterial OTUs that were highly abundant and distinct in each host species (Figs. 4b). Abundant alphaproteobacterial OTUs in *Suberites* sp. were assigned to the *Kilonielalles* order, while most of the abundant alphaproteobacterial OTUs in *Hymeniacidon* sp. were unclassified at the order level (Table S1). The separation of *A. cavernosa* and *S. carteri* from other sponge species along the second axis was related to the prevalence of a number of OTUs assigned to the Gammaproteobacteria class (Figs. 3b). *J. splendens* was also associated with two abundant OTUs assigned to the Gammaproteobacteria class and Chromatiales order (Fig. 4b).

Higher Taxon Abundance and OTU Compositional Analysis

The Proteobacteria was the most abundant phylum in all individual sponges of all species (average relative abundance 68.44 ± 19.05%) (Fig. 5). The Cyanobacteria was relatively abundant in all samples (9.30 ± 6.92%), with the exception of *Hymeniacidon* sp. and one sample of *Suberites* sp. Other abundant phyla included Chloroflexi (average relative abundance 1.28 ± 2.34%), Planctomycetes (1.13 ± 1.14%), Spirochaetes (1.44 ± 4.12%), Actinobacteria (4.59 ± 6.78%), Bacteroidetes (4.75 ± 3.16%), Euryarchaeota (2.03 ± 1.90%) and *Crenarchaeota* (2.72 ± 4.23%). In water samples, the most abundant phylum was also Proteobacteria. However, the relative abundance of Proteobacteria (44.20 ± 2.73%) was lower than that observed in most sponges with the exception of *A. cavernosa*. The second most abundant phylum in water

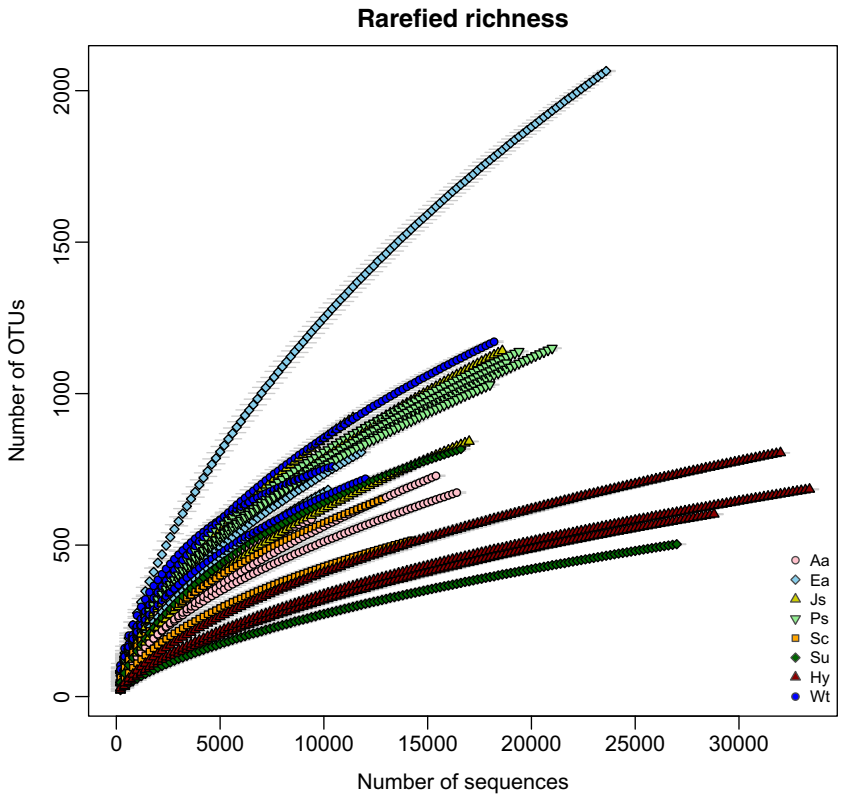

Fig. 2 Rarefied richness of the sponge-associated prokaryotic communities. *Aa Acanthella cavernosa*, *Ea Echinodictyum asperum*, *Js Jaspis splendens*, *Ps Ptilocaulis* sp., *Sc Stylissa carteri*, *Su Suberites* sp., *Hy Hymeniacidon* sp., *Wt* water

samples was Bacteroidetes (25.04 ± 5.64%). The relative abundance of Bacteriodetes was much higher in water than in all sponge species (Fig. 5). Other abundant phyla in water included Euryarchaeota (10.90 ± 4.37%), Actinobacteria (6.68 ± 1.76%) and Cyanobacteria (5.15 ± 1.97%) (Fig. 5).

The most abundant classes in sponge samples were Alphaproteobacteria (average relative abundance 29.94 ± 31.15%), Gammaproteobacteria (24.11 ± 3.53%), Synechococcophycidea (9.18 ± 6.85%), Betaproteobacteria (8.33 ± 1.37%), Deltaproteobacteria (5.81 ± 9.81%) and Flavobacteriia (3.89 ± 2.75%) (Fig. 6). In water samples, the most abundant classes were Alphaproteobacteria (26.95 ± 4.21%), Flavobacteriia (23.61 ± 5.94%), Gammaproteobacteria (15.40 ± 3.53%), Thermoplasmata (10.89 ± 4.36%) and Acidimicrobiia (6.51 ± 1.73%). In line with the PCO analysis, the most striking differences at the class level were related to the relative abundance of Alphaproteobacteria that was far higher in *Suberites* sp. (65.75 ± 4.93%) and in *Hymeniacidon* sp. (90.74 ± 3.23%) than in the remaining samples (15.38 ± 7.67%) (Fig. 6). Also in line with the PCO analysis (third and fourth axes, Fig. 4a, b), the heatmap analysis revealed that each sponge species

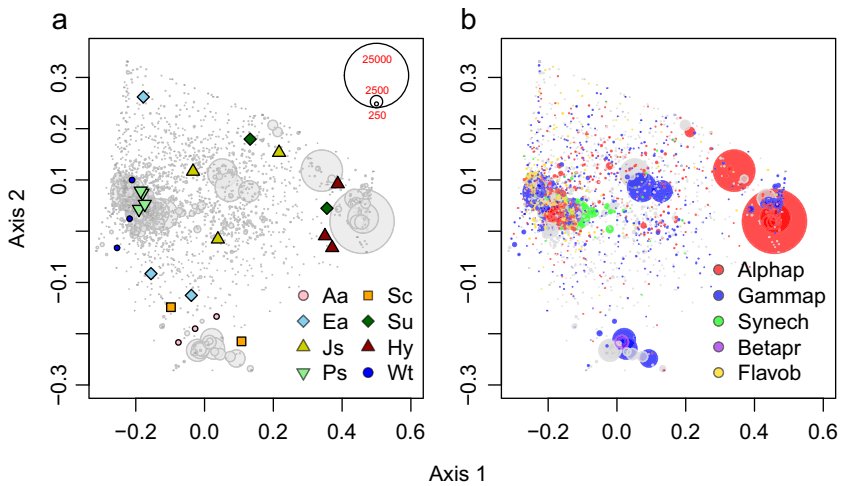

Fig. 3 Ordination showing the first two axes of the Principal Coordinates Analysis (PCO) of prokaryote OTU composition. **a** *Light grey symbols* represent operational taxonomic unit (OTU) scores with the symbol size representing their abundance (number of sequence reads). **b** The *color* of the symbol indicates their taxonomic affiliation (class level). *Aa Acanthella cavernosa*, *Ea Echinodictyum asperum*, *Js Jaspis splendens*, *Ps Ptilocaulis* sp., *Sc Stylissa carteri*, *Su Suberites* sp., *Hy Hymeniacidon* sp., *Wt* water

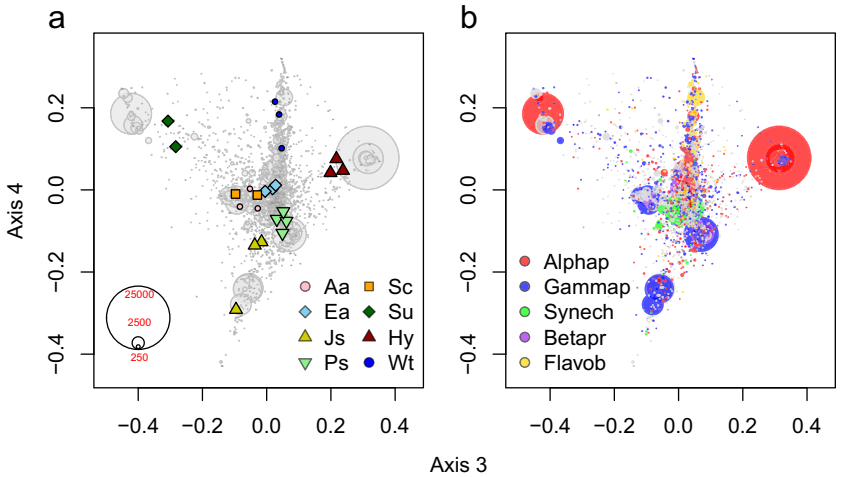

Fig. 4 Ordination showing the third and fourth axes of the Principal Coordinates Analysis (PCO) of prokaryote OTU composition. **a** *Light grey symbols* represent operational taxonomic unit (OTU) scores with symbol size representing their abundance (number of sequence reads). **b** The *color* of the symbol indicates their taxonomic affiliation (class level). *Aa Acanthella cavernosa*, *Ea Echinodictyum asperum*, *Js Jaspis splendens*, *Ps Ptilocaulis* sp., *Sc Stylissa carteri*, *Su Suberites* sp., *Hy Hymeniacidon sp.*, *Wt* water

was dominated by a limited set of OTUs (Fig. 7). *Acanthella cavernosa* was dominated by OTU-11 (average relative abundance 17.31 ± 4.70%). This OTU was assigned to the *Acidimicrobiales* order and had a sequence similarity of 94.37% with an organism retrieved from the LMA sponge *Poecillastra compressa* sampled in the northern Atlantic (Table S1). OTU-22 was another abundant OTU (10.30 ± 3.85%) in *A. cavernosa* (Fig. 7). This OTU was assigned to the *Crenarchaeota* phylum (*Archaea* domain) and had a sequence similarity of 99.51% with an organism obtained from the LMA sponge *Mycale laxissima* (Table S1). In *E. asperum*, OTU-7 (28.66 ± 12.26%), assigned to the betaproteobacterial order EC94, was the most abundant (Fig. 7) and had a sequence similarity of 95.32% with an organism obtained from the cold water sponge *Tsitsikamma favus* (Table S1). Other abundant OTUs in *E. asperum* included OTUs 10, 5 and 41 (7.95 ± 3.16%, 7.27 ± 2.40% and 7.20 ± 4.13%, respectively) (Fig. 7). OTUs 5 and 10 were assigned to the *Synechococcaceae* family. OTU 41 was similar (sequence similarity of 91.54%) to an organism obtained from the LMA sponge *Callyspongia vaginalis* (Table S1). *Jaspis splendens* samples were dominated by the deltaproteobacterial OTU 6 (25.60 ± 8.64%), and gammaproteobacterial (Chromatiales) OTUs 9 (24.49 ± 2.79%) and 19 (14.37 ± 9.64%) (Fig. 7). OTU-6 was similar to an organism obtained from a hypersaline basin (sequence similarity 95.1%, Table S1). OTU-9 was similar to an organism retrieved from the HMA sponge *Aplysina fulva* collected in the Caribbean Sea, and OTU-19 was similar to a sequence retrieved from river sediment (sequence similarity 95.98 and 92.86%, respectively, Table S1). *Ptilocaulis spiculifer* samples were dominated by OTUs 14, 15 and 10 (20.36 ± 3.95%, 10.81 ± 2.45% and 8.90 ± 1.78%) (Fig. 7) OTU-14, assigned to Gammaproteobacteria had high similarity (sequence similarity of 95.11%) with an organism retrieved from the LMA marine sponge *Raspailia topsenti* (Table S1). OTU 10 was assigned to the *Synechococcaceae* (Cyanobacteria phylum) and was similar (sequence similarity of 99.76%) to an organism retrieved from a hypersaline sediment. OTU 15 was assigned to the order EC94 and was similar (sequence similarity of 95.91%) to an organism retrieved from the LMA sponge *Haliclona* sp. (Table S1). In *Suberites* sp., OTU 3, assigned to the Alphaproteobacteria, dominated the prokaryote community (57.51 ± 1.80%) (Fig. 7). This OTU was assigned to the Kiloniellales order and was similar (sequence similarity 98.12%) to an organism collected in marine reef sediment (Table S1). *Stylissa carteri* was dominated by OTUs 16, 24 and 46 (25.00 ± 3.30%, 15.48 ± 13.78%, 7.00 ± 2.46%) (Fig. 7). These OTUs were assigned to the orders Chromatiales, Thiohalorhabdales and NB1-j, respectively. These OTUs were similar to organisms retrieved from the LMA sponges *Axinella* sp., *Phakellia fusca* and *Stylissa cartieri* (sequences similarities of 99.11, 97.99 and 99.55%, respectively). Samples of *Hymeniacidon* sp. were dominated by OTU 1 (64.62 ± 4.43) (Fig. 7). This OTU was assigned to the Alphaproteobacteria class and was similar (sequence similarity = 97.64%) to an organism retrieved from the sponge *Tedania ignis* originally collected in a mangrove in the Caribbean Sea (Table S1). OTUs 6735, 6896, 11,947 and 747 assigned to the Alphaproteobacteria were almost exclusively found in *Hymeniacidon* sp. (14.69 ± 1.03, 2.82 ± 0.72, 3.11 ± 0.58 and 2.14 ± 0.54) (Fig. 7). OTUs 6735, 747 and 11,947 were similar (sequences similarities 98.35%, 98.11% and 97.64%, respectively) to organisms retrieved from *Hymeniacidon pervelis* in the intertidal zone of Ballyhenry Island, Ireland (Table S1). OTU 6896 was similar to an organism retrieved from *Terpios hoshinota* collected in China (sequence similarity 98.11%) (Table S1).

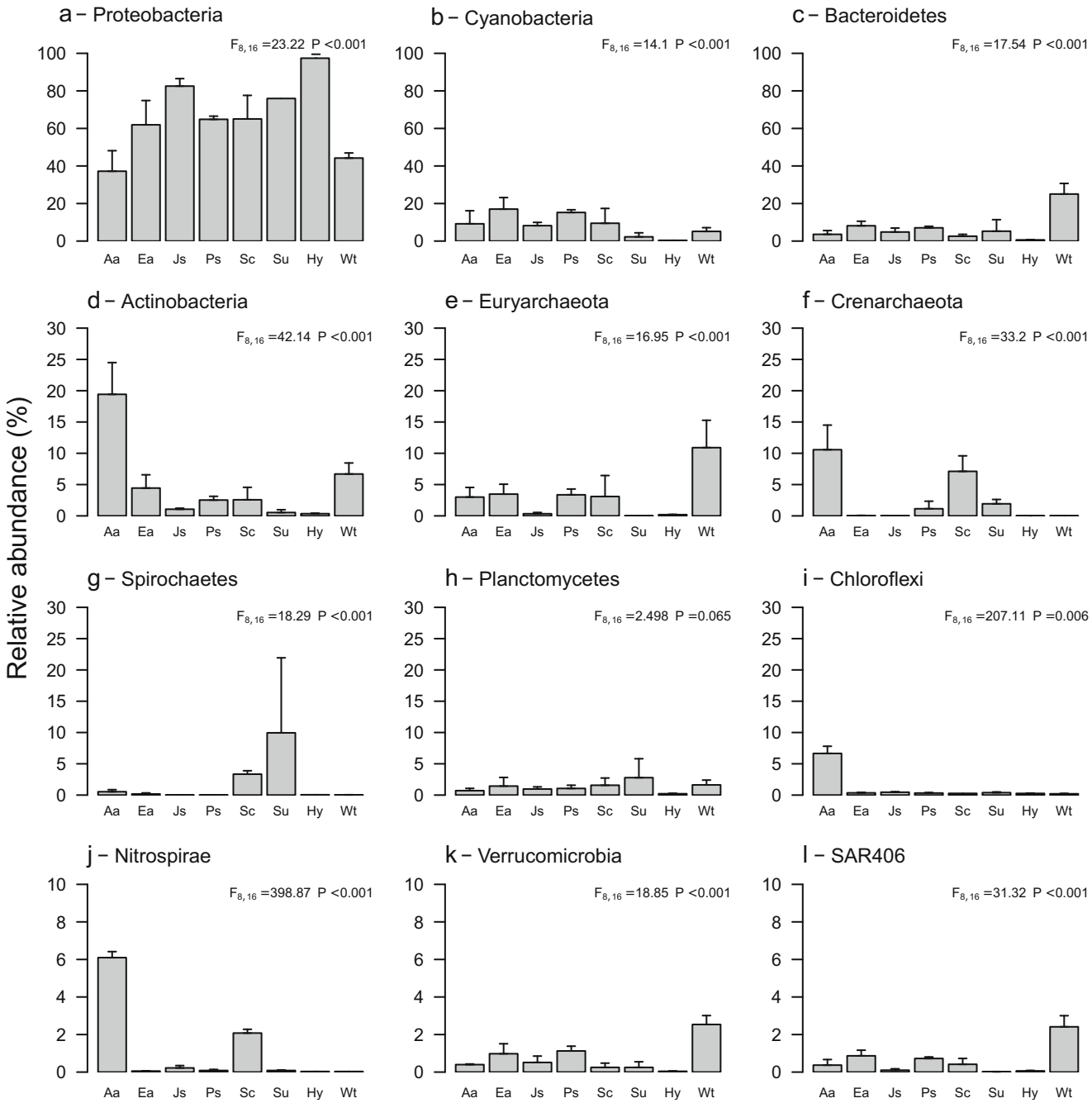

Fig. 5 Relative abundance of the most abundant prokaryote phyla for samples from *Aa Acanthella cavernosa*, *Ea Echinodictyum asperum*, *Js Jaspis splendens*, *Ps Ptilocaulis* sp., *Sc Stylissa carteri*, *Su Suberites* sp., *Hy Hymeniacidon* sp., *Wt* water

In water samples, the dominance of the most abundant OTU was much lower than in sponge samples (Fig. 6a). In line with the PCO (first and second axes, Fig. 3a, b), the heatmap analysis also revealed a close association of samples from water and samples from *E. asperum* and *P. spiculifer* (Fig. 7). With the exception of OTUs 5 and 10, assigned to the phylum Cyanobacteria, this association was not related to the dominant OTUs of each sponge.

Alphaproteobacteria Phylogeny

Taking into account the pronounced differences in the relative abundance of the Alphaproteobacteria class in different sponge species, we focused our phylogenetic analysis on dominant OTUs assigned to this class. In the phylogenetic tree (Fig. S1), there were three main clusters. OTUs 90, 31 and 61 were included in a weekly supported cluster together with Alphaproteobacteria sequences found in water, in sediment and

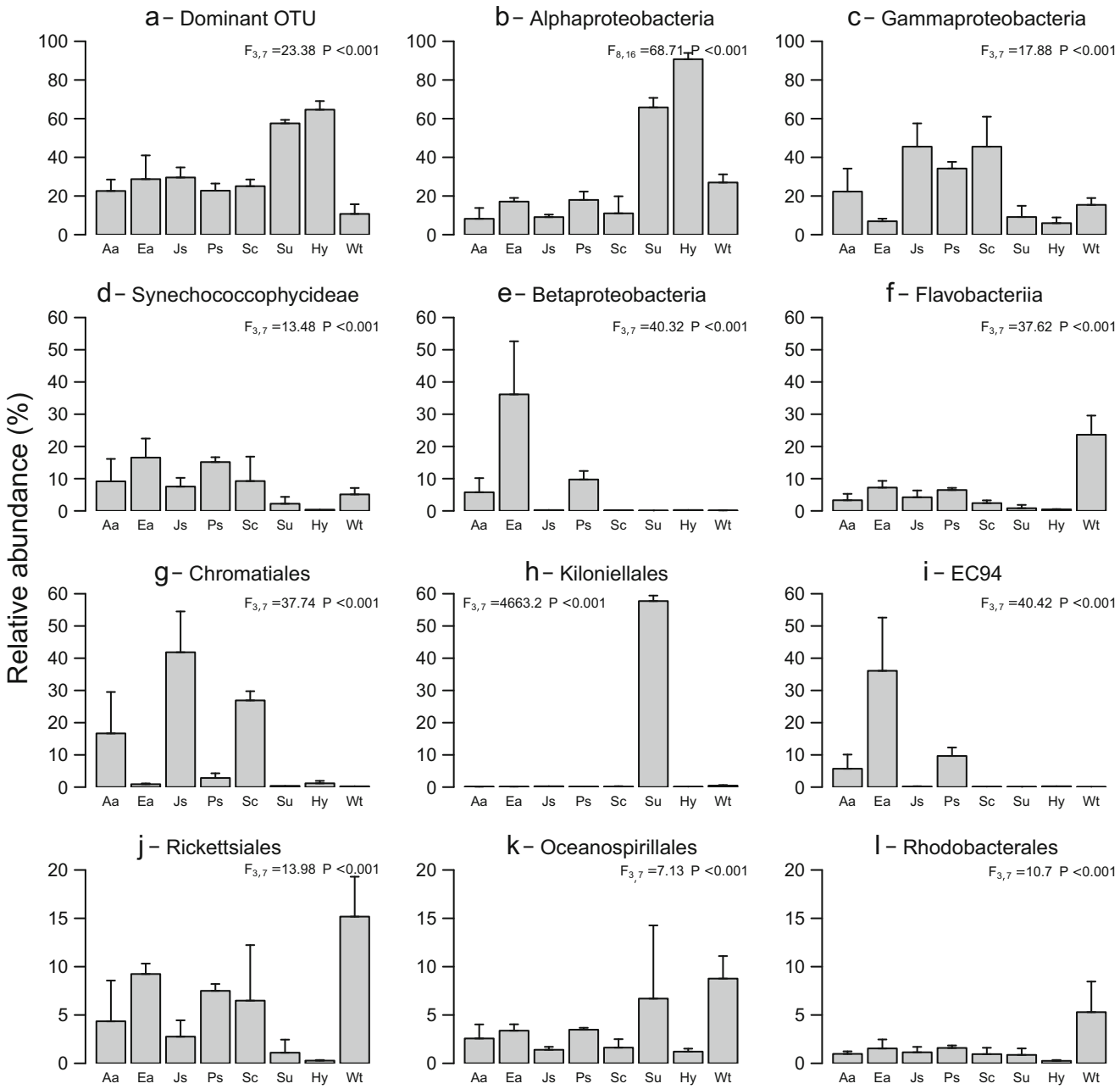

Fig. 6 Relative abundance of the most abundant prokaryote classes, orders and the dominant OTU for samples from *Aa Acanthella cavernosa*, *Ea Echinodictyum asperum*, *Js Jaspis splendens*, *Ps Ptilocaulis* sp., *Sc Stylissa carteri*, *Su Suberites* sp. and *Hy Hymeniacidon* sp., *Wt* water

in *Hymeniacidon heliophila* collected in the subtidal zone in the study by Weigel and Erwin [40] (Fig. S1). Only one Alphaproteobacteria found in *H. heliophila* collected in the intertidal zone was included in this first cluster. The second cluster included OTU 3 that dominated the prokaryotic community of *Suberites* sp. and alphaproteobacterial sequences collected in the study by Clearly [8]. A third cluster was divided in two subclusters (i) containing OTU 126 and alphaproteobacterial sequences found in *H. heliophila* collected in the intertidal zone in the study by Weigel and Erwin [40] and (ii) consisting of OTUs that dominated the prokaryote community of *Hymeniacidon* sp. (OTUs 1, 747, 6735, 6896 and 11,947), alphaproteobacterial sequences found in seawater from an area surrounding *Hymeniacidon perlevis* and alphaproteobacterial sequences found in *H. heliophila* collected in the intertidal zone [40].

Predictive Gene Enrichment

For some species, we were unable to collect more than two samples. For the predictive gene analysis, we focused only on water and sponge samples that had at least three replicates, namely, *A. cavernosa*, *E. asperum*, *J. splendens*, *Ptilocaulis* sp. and

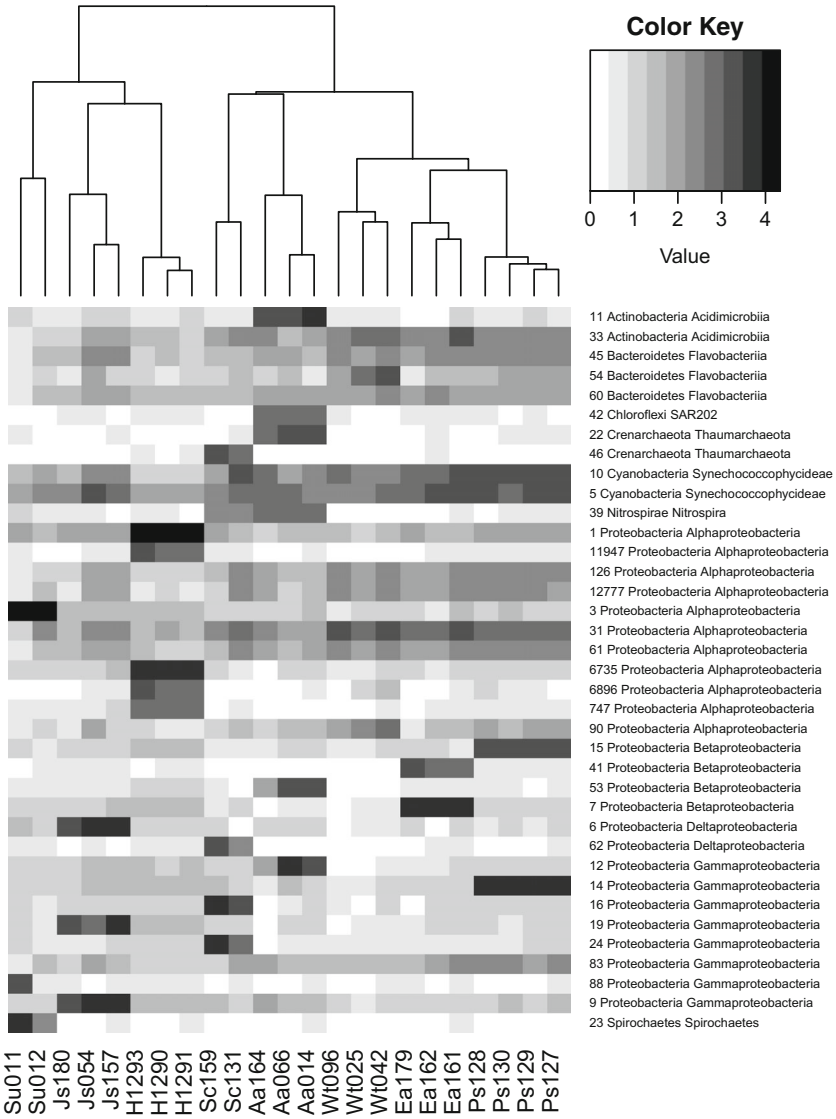

Fig. 7 Heatmap showing the abundance of dominant OTUs (sequence reads ≥1500 sequences). The heatmap was generated using the function heatmap2() in the R package gplots (http://www.cran.r-project.org/). The OTUs were log-transformed and clustered according to their occurrence by UPGMA hierarchical clustering. *Aa Acanthella cavernosa*, *Ea Echinodictyum asperum*, *Js Jaspis splendens*, *Ps Ptilocaulis* sp., *Sc Stylissa carteri*, *Su Suberites* sp., *H Hymeniacidon sp.*, *Wt* water

Hymeniacidon sp. Samples of *Hymeniacidon* sp. had the lowest NSTI (0.08 ± 0.0005) indicating that the sequences obtained from this sponge were closely related to sequences in the reference metagenome database. *Acanthella cavernosa* had the highest NSTI values (0.17 ± 0.03). A PCO analysis of KEGG ortholog (KO) composition showed a separation between sponge samples collected in the coral reef habitat and water versus samples collected in the hydrothermal habitat (Fig. S2). Adonis analysis further confirmed a significant difference in KO composition between water and coral reef and hydrothermal samples (adonis, $F_{1,18} = 14.217$, $R^2 = 0.455$, $P = 0.001$). Assessment of the most abundant pathways (KEGG level 2) supported this observation, with several predicted pathways enriched in samples of *Hymeniacidon* sp. (Fig. S3). In particular, there was pronounced predicted enrichment in samples of *Hymeniacidon* sp. in the replication and repair (9.20 ± 0.03) category when compared with the rest of the sponge (7.66 ± 0.23) and water samples (7.49 ± 0.14). Considering the extreme nature of the hydrothermal vent habitat, we further focused our analysis on specific replication and repair pathways. There were several pathways classified within this category that showed higher relative abundances in samples of *Hymeniacidon* sp. when compared to other samples (Fig. 8). The pathways DNA repair and recombination proteins, chromosome, DNA replication proteins, homologous recombination, mismatch repair, DNA replication and base excision repair were all significantly higher (Fig. 8) in samples of *Hymeniacidon* sp. (2.97 ± 0.01%, 1.58 ± 0.004%, 1.27 ± 0.006%, 0.97 ± 0.003%, 0.82 ± 0.003%, 0.71 ± 0.003% and 0.51 ± 0.002%, respectively) than in the rest of the sponge species (average relative abundance 2.55 ± 0.07%, 1.26 ± 0.04%, 0.96 ± 0.04%, 0.81 ± 0.04%, 0.66 ± 0.003%, 0.58 ± 0.03% and 0.45 ± 0.04%, respectively) and water (2.48 ± 0.04%, 1.24 ± 0.04%, 1.00 ± 0.01%, 0.75 ± 0.03%, 0.61 ± 0.02%, 0.58 ± 0.01% and 0.45 ± 0.008%). We also analysed in detail the amino acid metabolism specific pathways (Fig. 9). Several of

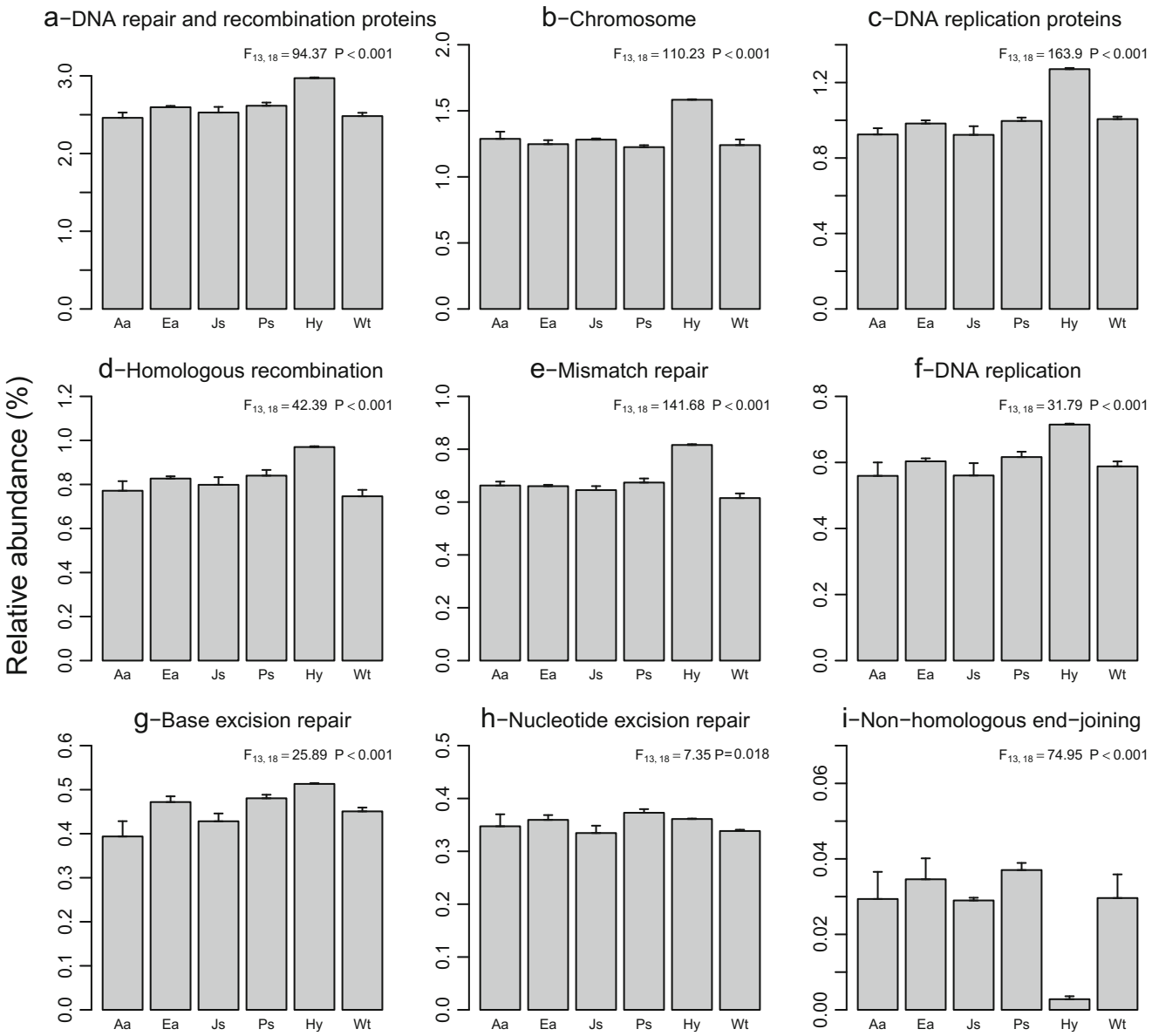

Fig. 8 Mean relative gene count abundance of pathways involved in the replication and repair subcategory for samples from *Aa Acanthella cavernosa*, *Ea Echinodictyum asperum*, *Js Jaspis splendens*, *Ps Ptilocaulis* sp., Hy Hymeniacidon sp and *Wt* water. *Error bars* represent a single standard deviation. The pathways shown include the following: DNA repair and recombination proteins, chromosome, DNA replication proteins, homologous recombination, mismatch repair, DNA replication, base excision repair, nucleotide excision repair and non-homologous end-joining

these pathways were also enriched in *Hymenacidon* sp. when compared to the rest to the sponge species. The relative gene content of the glycine, serine and threonine metabolism, amino acid-related enzymes, alanine, aspartate and glutamate metabolism, lysine biosynthesis, phenylalanine metabolism, valine, leucine and isoleucine degradation and tryptophan metabolism pathways were significantly higher in *Hymeniacidon* sp. (1.57 ± 0.01%, 1.64 ± 0.01%, 1.13 ± 0.004%, 0.77 ± 0.003%, 0.31 ± 0.0004%, 0.82 ± 0.0004%, 0.61 ± 0.0004%, respectively) than in the other sponge species (1.06 ± 0.09%, 1.43 ± 0.07%, 1.00 ± 0.04%, 0.71 ± 0.03%, 0.27 ± 0.013%,0.63 ± 0.05% and 0.43 ± 0.04%, respectively) and water (1.24 ± 0.03, 1.43 ± 0.01%, 1.05 ± 0.01%, 0.70 ± 0.02%, 0.32 ± 0.03%, 0.85 ± 0.10%, 0.57 ± 0.07%, respectively). On the other hand, the relative gene count of the arginine and proline metabolism and histine and tyrosine metabolism pathways were significantly lower in *Hymeniacidon* sp. (1.11 ± 0.0007%, 0.43 ± 0.001% and 0.22 ± 0.002%, respectively) than in the other sponge species (1.37 ± 0.059%, 0.66 ± 0.04% and 0.38 ± 0.02%, respectively) and water (1.37 ± 0.01%,0.67 ± 0.04% and 0.44 ± 0.01%, respectively).

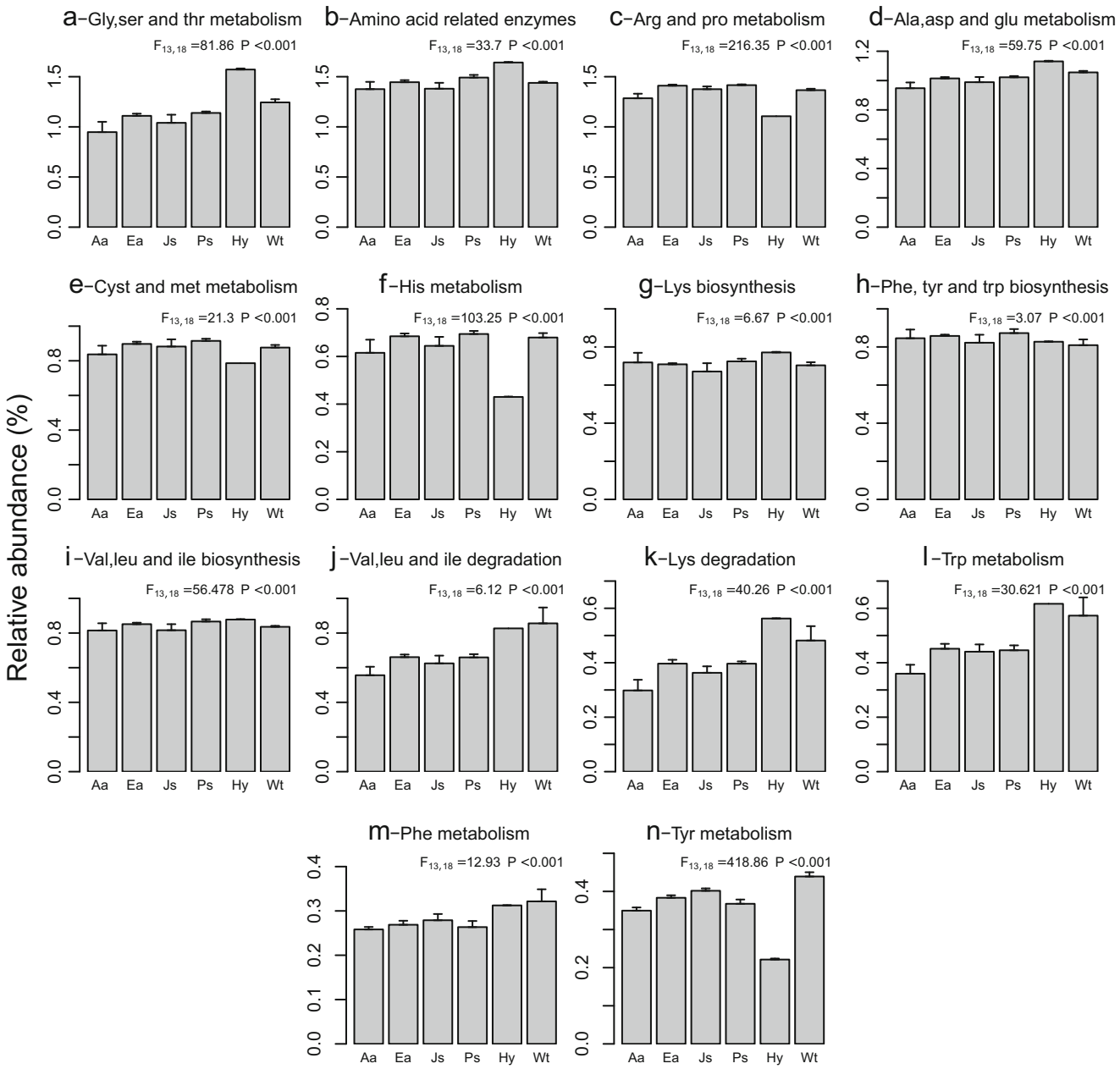

Fig. 9 Mean relative abundance of pathways involved in the amino acid metabolism subcategory for samples from *Aa Acanthella cavernosa*, *Ea Echinodictyum asperum*, *Js Jaspis splendens*, *Ps Ptilocaulis* sp., *Hy Hymeniacidon* sp and *Wt* Water. *Error bars* represent a single standard deviation. The pathways shown include the following: glycine, serine and threonine metabolism; amino acid-related enzymes; arginine and proline metabolism; alanine, aspartate and glutamate metabolism; cysteine and methionine metabolism; histidine metabolism; lysine biosynthesis; phenylalanine, tyrosine and tryptophan biosynthesis; valine, leucine and isoleucine biosynthesis; valine, leucine and isoleucine degradation; lysine degradation; tryptophan metabolism; phenylalanine metabolism; and tyrosine metabolism

Discussion

As expected, OTUs assigned to the phylum Proteobacteria were an abundant component of all sponge species. LMA sponges are generally characterized by low phylum-level diversity, with a preponderance of Proteobacteria [14]. The preponderance of OTUs assigned to the Alpha- and Gammaproteobacteria is consistent with recent sponge microbiome surveys [3]. Also consistent with recent surveys, was the dominance of a limited set of OTUs in each sponge species, which contrasts with the samples from nearby water collected in this study and with HMA sponges that are generally characterized by a more even community [41]. The close association of water samples with *E. asperum* and *P. spiculifer*, was probably related to the presence of transient OTUs, that occurred in all the sponges but at a higher abundance in these two species. With the exception of samples of *J. splendens*, all host sponge species had dominant OTUs,

which were similar to sequences of organisms previously obtained from other LMA sponges. In the specific case of *J. splendens*, it is noteworthy that all the dominant OTUs had a relatively low similarity with BLAST matches. Overall, the dominance pattern is in line with recent studies that showed that LMA sponges have lower phylum-level diversity than HMA sponges and are dominated by relatively few OTUs [42]. Blanquer et al. also showed that the microbial community of a set of Mediterranean sponges was primarily defined by their affiliation to the HMA or LMA group rather than to host phylogeny or environmental conditions [42]. The maintenance of sponge-enriched symbionts occurs either directly through vertical transmission, horizontally through acquisition from the surrounding water or through a combination of both strategies [43]. The similarity of these OTUs to sequences obtained from other LMA sponge species in disparate geographical areas indicates intimate host-symbiont associations that may possibly be maintained through vertical transmission. However, we cannot exclude the hypothesis of recruitment from the rare biosphere of seawater. Recent studies have shown that sponges may also acquire their symbionts within the rare biosphere in addition to vertical transmission [44]. Despite all of the LMA sponges in this study having a pronounced dominance of a limited set of OTUs, the PCO analysis clearly showed that both *Suberites* sp. and *Hymeniacidon* sp. were the most distinct when compared to the other sponge species. These compositional differences were related to the occurrence of distinct OTUs assigned to the Alphaproteobacteria in both sponge species. Cleary et al. (2013) previously reported on the pronounced dominance of Alphaproteobacteria in samples of *Suberites diversicolor* from the marine lakes of Berau, Indonesia [8]. The dominant OTUs in *Suberites diversicolor* were also assigned to the recently described order Killelionales [45] as was the case with *Suberites* sp. in the present study. Our phylogenetic tree, furthermore, demonstrated a strong phylogenetic relationship between the dominant OTU retrieved in this study and the OTUs assigned to the Killelionales order in the study of Cleary et al. (2013) (Fig. S1). In the specific case of *Hymeniacidon sp*., alphaproteobacterial dominance could be related to the specific conditions of the hydrothermal habitat such as reduced pH levels or with the reduced chemical species that are vented at the hydrothermal system. Meron et al. (2011) reported an increase in coral associated alphaproteobacterial sequences under reduced seawater pH levels consistent with ocean acidification scenarios (7.3) [46]. Interestingly, the marine lakes of Berau (Haji Buang and Kakaban lakes) East Kalimantan Province, Indonesia from which *S. diversicolor* samples were collected [8] also had a lower pH level (7.3–7.8 and 7.0–7-8, respectively) than seawater [47]. On the other hand, this increase could be related to the specific hydrothermal chemical conditions since recent isolates assigned to this family are able to oxidize sulfur and hydrogen and were isolated at a hydrothermal field on the Mid-Atlantic Ridge [48].

The phylogenetic tree demonstrated that alphaproteobacterial OTUs from *Hymeniacidon* sp. formed a distinct cluster including an OTU detected from water samples surrounding *Hymeniacidon* sp. in an intertidal zone (Fig. S1—OTUs 1, 747, 11,947, 6735, and 6896). This cluster included *Nisaea nitritireducens*, a species potentially involved in denitrification and classified within the order Rhodospirillales [49]. Interestingly, a recent study by Weigel and Erwin (2016), reported a higher preponderance of alphaproteobacterial OTUs in specimens of *Hymeniacidon heliophila* in the more stressful intertidal zone than sponges of the same species collected in the subtidal zone [40]. We included sequences classified as Alphaproteobacteria retrieved from Weigel and Erwin [40] in our phylogenetic tree. Interestingly, two OTUs retrived from *Hymeniacidon heliophila* and collected in the intertidal zone clustered together with the OTUs from *Hymeniacidon* sp. in our study (Fig. S1). Although the intertidal zone and the hydrothermal habitat are clearly distinct, sponges from the both habitats are subject to oxidative stress. In the specific case of the intertidal zone, the high levels of ultraviolet radiation (UV) induce oxidative cell damage. In the hydrothermal habitat, the abundance of hydrogen sulfide (H_2S) and oxygen leads to the oxidation of H_2S and the production of oxygen and sufur-centered radicals [50]. It is believed that the high tolerance of *Hymeniacidon heliophila* to oxidative stress induced by UV is linked to the production of L-5-hydroxytryptophan, a strong antioxidant that is found in high concentrations in this sponge species [51].

PICRUSt results should be interpreted with caution, since the predicted metagenome is dependent on the available sequenced genomes and some bias can be produced if reference species are missing. To account for such biases, the software includes methods for quality control to test the reliability of the predictions. The NSTI values quantify the availability of nearby genome representatives for each sample and can be used to evaluate predictive accuracy (https://picrust.github.io). The lower the NSTI values, the more accurate are the predictions. Langille et al. (2013) showed that the best results were obtained for Human Microbiome Project samples (mean NSTI 0.003), mid-range for a data set of soil samples (mean NSTI 0.17) and highest for poorly explored environment (mean NSTI 0.23). In the present study, NSTI scores varied from 0.08 ± 0.0005 for *Hymeniacidon* sp. to 0.17 ± 0.03 from *A. cavernosa*. These values are within what can be considered a moderate coverage range. Soil samples with NSTI values within this range (mean NSTI 0.17) have been shown to provide accurate metagenome predictions with PICRUSt [38].

The predicted functional analysis revealed a clear distinction between the metagenome profile of sponge samples collected in the coral reef and those collected in the shallow

hydrothermal vent. The prokaryote community of *Hymeniacidon* sp. was characterized by a higher relative abundance of KOs assigned to replication and repair and translation pathways. The enrichment of KOs assigned to replication and repair pathways was most likely linked to the hydrothermal extreme environment. For example, within replication and repair, there was enrichment for KOs assigned to the base excision repair pathway (Fig. 8g) that is involved in DNA repair from damage induced by hydrolysis, reactive oxygen species and other metabolites that alter DNA structure [52]. As another example, also within replication and repair, KOs assigned to the mismatch and repair pathway were also enriched (Fig. 8e). The mismatch and repair pathway also plays a key role in maintaining genomic stability and correcting DNA mismatches generated during DNA replication [53]. In line with this observation, Xie et al. (2011) compared two deep-sea hydrothermal vent chimney microbiomes and found that they were both enriched for genes associated with mismatch repair and homologous recombination. This further supports the link between the high relative abundance of KOs assigned to replication and repair and the harsh conditions of the hydrothermal vent habitat [54]. Interestingly, the genes associated with non-homologous end-joining, an error-prone pathway [55], were significantly reduced in samples of *Hymeniacidon* sp.

The predictive gene metagenome also revealed enrichment in KOs assigned to the amino acid metabolism. When compared with the rest of the sponges, samples of *Hymeniacidon* sp. were characterized by a high relative abundance of KOs assigned to the tryptophan metabolism (Fig. 9l), a precursor of L-5-hydroxytryptophan, that, as mentioned previously, plays a fundamental role in the resistance to oxidative stress. The prokaryote community of *Hymeniacidon* sp. could be involved in the metabolism of this antioxidant compound.

Conclusion

In this study, we characterized the structure and putative function of prokaryotic communities from LMA sponges collected in two highly contrasting ecosystems (coral reef and hydrothermal vent) but in the same geographical area (vicinal islands of Taiwan). Our results showed that the sponge species collected in the hydrothermal vent habitat had a highly distinct prokaryote community and putative function presumably related to coping with the chronic stress associated with the vent environment. Recently, Morrow et al. (2015) suggested that some sponge species are able to acquire microbial symbionts that enable them to survive in harsh conditions such as high pCO_2 levels that naturally occur within volcanic CO_2 seeps [56]. Such a relationship could also play a role in the survival of LMA sponges under extreme environments.

Acknowledgements Thanks are due, for the financial support to CESAM (UID/AMB/50017/2013), to FCT/MEC through national funds, and the co-funding by the FEDER, within the PT2020 Partnership Agreement and Compete 2020. This work was also supported by the projects LESS CORAL (PTDC/AAC-AMB/115304/2009) and EcotechSponge (PTDC/BIA-MIC/6473/2014 - POCI-01-0145-FEDER-016531) Thank are also due to the Ministry of Science and Technology (MOST), Taiwan under grant NSC 102-2815-C-346-010-B and the Asia-Pacific Ocean Research Center, National Sun Yat-sen University, supported by the Ministry of Education, Taiwan. Francisco J. R. C. Coelho was supported by a postdoctoral scholarship (SFRH/BPD/92366/2013) financed by the Portuguese Foundation for Science and Technology. We are grateful for the support in the field by Julian Cleary, Floris Cleary and Katherine Liao.

References

1. McFall-Ngai M, Hadfield MG, Bosch TCG, Carey HV, Domazet-Lošo T, Douglas AE, Dubilier N, Eberl G, Fukami T, Gilbert SF, Hentschel U, King N, Kjelleberg S, Knoll AH, Kremer N, Mazmanian SK, Metcalf JL, Nealson K, Pierce NE, Rawls JF, Reid A, Ruby EG, Rumpho M, Sanders JG, Tautz D, Wernegreen JJ (2013) Animals in a bacterial world, a new imperative for the life sciences Proc Natl Acad Sci U S A 110:3229–3236. doi:10.1073/pnas.1218525110
2. Woyke T, Teeling H, Ivanova NN, Huntemann M, Richter M, Gloeckner FO, Boffelli D, Anderson IJ, Barry KW, Shapiro HJ, Szeto E, Kyrpides NC, Mussmann M, Amann R, Bergin C, Ruehland C, Rubin EM, Dubilier N (2006) Symbiosis insights through metagenomic analysis of a microbial consortium Nature 443:950–955 http://www.nature.com/nature/journal/v443/n7114/suppinfo/nature05192_S1.html
3. Thomas T, Moitinho-Silva L, Lurgi M, Bjork JR, Easson C, Astudillo-Garcia C, Olson JB, Erwin PM, Lopez-Legentil S, Luter H, Chaves-Fonnegra A, Costa R, Schupp PJ, Steindler L, Erpenbeck D, Gilbert J, Knight R, Ackermann G, Victor Lopez J, Taylor MW, Thacker RW, Montoya JM, Hentschel U, Webster NS (2016) Diversity, structure and convergent evolution of the global sponge microbiome Nat Commun 7:11870. doi:10.1038/ncomms11870
4. Taylor MW, Radax R, Steger D, Wagner M (2007) Sponge-associated microorganisms: evolution, ecology, and biotechnological potential Microbiol Mol Biol Rev 71:295–347. doi:10.1128/mmbr.00040-06
5. Wilkinson CR (1983) Net primary productivity in coral reef sponges Science 219:410–412. doi:10.1126/science.219.4583.410
6. Hochmuth T, Piel J (2009) Polyketide synthases of bacterial symbionts in sponges—evolution-based applications in natural products research Phytochemistry 70:1841–1849. doi:10.1016/j.phytochem.2009.04.010
7. Piel J (2009) Metabolites from symbiotic bacteria Nat Prod Rep 26:338–362. doi:10.1039/B703499G
8. Cleary DFR, Becking LE, NJd V, ACC P, ARM P, Egas C, NCM G (2013) Habitat- and host-related variation in sponge bacterial symbiont communities in Indonesian waters FEMS Microbiol Ecol 85:465–482. doi:10.1111/1574-6941.12135
9. Cleary DFR, de Voogd NJ, Polónia ARM, Freitas R, Gomes NCM (2015) Composition and predictive functional analysis of bacterial communities in seawater, sediment and sponges in the Spermonde archipelago, Indonesia Microb Ecol 70:889–903. doi:10.1007/s00248-015-0632-5
10. de Voogd NJ, Cleary DFR, Polónia ARM, Gomes NCM (2015) Bacterial community composition and predicted functional ecology

of sponges, sediment and seawater from the thousand islands reef complex, West Java, Indonesia. FEMS Microbiol Ecol 91. doi:10.1093/femsec/fiv019

11. Erwin PM, Coma R, López-Sendino P, Serrano E, Ribes M (2015) Stable symbionts across the HMA-LMA dichotomy: low seasonal and interannual variation in sponge-associated bacteria from taxonomically diverse hosts. FEMS Microbiol Ecol 91. doi:10.1093/femsec/fiv115
12. Hentschel U, Piel J, Degnan SM, Taylor MW (2012) Genomic insights into the marine sponge microbiome Nat Rev Microbiol 10:641–654
13. Vacelet J, Donadey C (1977) Electron microscope study of the association between some sponges and bacteria J Exp Mar Biol Ecol 30:301–314. doi:10.1016/0022-0981(77)90038-7
14. Giles EC, Kamke J, Moitinho-Silva L, Taylor MW, Hentschel U, Ravasi T, Schmitt S (2013) Bacterial community profiles in low microbial abundance sponges FEMS Microbiol Ecol 83:232–241. doi:10.1111/j.1574-6941.2012.01467.x
15. Hoeksema B (2007) Delineation of the Indo-Malayan centre of maximum marine biodiversity: the coral triangle. In: Renema, W (ed) Biogeography in time and place: Distributions, barriers and islands, Netherlands, pp 117–178
16. Veron JEN, Devantier LM, Turak E, Green AL, Kininmonth S, Stafford-Smith M, Peterson N (2009) Delineating the Coral Triangle, Galaxea J Coral Reef Stud 11:91–100. doi:10.3755/galaxea.11.91
17. Hsieh HJ, Chen CA, Dai C-F, Ou W, Tsai W-S, Su W-C (2007) From the drawing board to the field: an example for establishing an MPA in Penghu, Taiwan Aquat Conserv 17:619–635. doi:10.1002/aqc.826
18. Huang YM, de Voogd NJ, Cleary DFR, Li T-H, Mok H-K, Ueng J-P (2016) Biodiversity pattern of subtidal sponges (Porifera: Demospongiae) in the Penghu Archipelago (Pescadores), Taiwan J Mar Biol Assoc UK 96:417–427. doi:10.1017/S002531541500017X
19. Kuo F-L, Huang Y (2015) The biodiversity and distribution of subtidal sponges (Porifera) in the South Penghu Marine National Park, Taiwan. Marine National Park Headquarters
20. Chentung AC, Bingjye W, Jungfu H, Jiannyuh L, Fuwen K, Yuehyuan T, Hsienshiow T (2005) Investigation into extremely acidic hydrothermal fluids off Kueishan Tao, Taiwan, China. Chinese Society of Oceanography, Beijing
21. Chen C-TA, Zeng Z, Kuo F-W, Yang TF, Wang B-J, Tu Y-Y (2005) Tide-influenced acidic hydrothermal system offshore NE Taiwan Chem Geol 224:69–81. doi:10.1016/j.chemgeo.2005.07.022
22. Tsai T-L, Liu S-M, Lee S-C, Chen W-J, Chou S-H, Hsu T-C, Guo G-L, Hwang W-S, Wiegel J (2011) Ethanol production efficiency of an anaerobic hemicellulolytic thermophilic bacterium, strain NTOU1, isolated from a marine shallow hydrothermal vent in Taiwan Microbes Environ 26:317–324. doi:10.1264/jsme2.ME10202
23. Wang L, Cheung MK, Kwan HS, Hwang J-S, Wong CK (2015) Microbial diversity in shallow-water hydrothermal sediments of Kueishan Island, Taiwan as revealed by pyrosequencing J Basic Microbiol 55:1308–1318. doi:10.1002/jobm.201400811
24. Jeng M-S, Clark PF, Ng PKL (2004) The first zoea, megalopa, and first crab stage of the hydrothermal vent crab *Xenograpsus testudinatus* (Decapoda: Brachyura: Grapsoidea) and the systematic implications for the Varunidae J Crustac Biol 24:188–212
25. Chen Y-G, Liu T-K (1996) Sea level changes in the last several thousand years, Penghu Islands, Taiwan Strait Quat Res 45:254–262. doi:10.1006/qres.1996.0026
26. Liao E, Jiang Y, Li L, Hong H, Yan X (2013) The cause of the 2008 cold disaster in the Taiwan Strait Ocean Model 62:1–10. doi:10.1016/j.ocemod.2012.11.004
27. Chen C-TA, Wang B-J, Huang JF, Lou JY, Kuo FW, Tu Y-Y, Tsai HS (2005) Investigation into extremely acidic hydrothermal fluids off Kueishantao Islet, Taiwan Acta Oceanol Sin 24:125–133
28. Caporaso JG, Kuczynski J, Stombaugh J, Bittinger K, Bushman FD, Costello EK (2010) QIIME allows analysis of high-throughput community sequencing data. Nat Methods 7:335–336
29. Edgar RC (2013) UPARSE: highly accurate OTU sequences from microbial amplicon reads Nat Methods 10:996–998. doi:10.1038/nmeth.2604
30. Edgar RC, Haas BJ, Clemente JC, Quince C, Knight R (2011) UCHIME improves sensitivity and speed of chimera detection Bioinformatics 27:2194–2200. doi:10.1093/bioinformatics/btr381
31. Wang Q, Garrity G, Tiedje J, Cole J (2007) Naive Bayesian classifier for rapid assignment of rRNA sequences into the new bacterial taxonomy Appl Environ Microbiol 73:5261–5267
32. R Core Team (2013) R: A Language and Environment for Statistical Computing. R Foundation for Statistical Computing, Vienna, Austria ISBN 3-900051-07-0. Available from http://www.Rproject.orghttp://www.R-project.org
33. Zhang Z, Schwartz S, Wagner L, Miller W (2000) A greedy algorithm for aligning DNA sequences J Comput Biol 7:203–214. doi:10.1089/10665270050081478
34. Gomes NCM, Cleary DFR, Pinto FN, Egas C, Almeida A, Cunha A, Mendonça-Hagler L CS, Smalla K (2010) Taking root: enduring effect of rhizosphere bacterial colonization in mangroves. PLoS One 5: e14065. doi:10.1371/journal.pone.0014065
35. Oksanen J, Guillaume Blanchet F, Kindt R, Legendre P, Minchin PR, O'Hara RB, Simpson GL, Solymos P, Henry H, Stevens M, Wagner H (2012). vegan: Community Ecology PackageR package version 20–3. https://cran.r-project.org/package=vegan
36. Martins P, Cleary DFR, Pires ACC, Rodrigues AM, Quintino V, Calado R, Gomes NCM (2013) Molecular analysis of bacterial communities and detection of potential pathogens in a recirculating aquaculture system for *Scophthalmus maximus* and *Solea senegalensis* PLoS One 8:e80847. doi:10.1371/journal.pone.0080847
37. Tamura K, Stecher G, Peterson D, Filipski A, Kumar S (2013) MEGA6: Molecular Evolutionary Genetics Analysis Version 6.0 Mol Biol Evol 30:2725–2729. doi:10.1093/molbev/mst197
38. Langille MG, Zaneveld J, Caporaso JG, McDonald D, Knights D, Reyes JA (2013) Predictive functional profiling of microbial communities using 16S rRNA marker gene sequences Nat Biotechnol 31:814–821
39. Coelho FJRC, Cleary DFR, Rocha RJM, Calado R, Castanheira JM, Rocha SM, Silva AMS, Simões MMQ, Oliveira V, Lillebø A, Almeida A, Cunha Â, Lopes I, Ribeiro R, Moreira-Santos M, Marques CR, Costa R, Pereira R, Gomes NCM (2015) Unraveling the interactive effects of climate change and oil contamination on laboratory simulated estuarine benthic communities Glob Chang Biol 21:1871–1886. doi:10.1111/gcb.12801
40. Weigel BL, Erwin PM (2016) Intraspecific variation in microbial symbiont communities of the sun sponge, *Hymeniacidon heliophila*, from intertidal and subtidal habitats Appl Environ Microbiol 82:650–658. doi:10.1128/AEM.02980-15
41. Cárdenas CA, Bell JJ, Davy SK, Hoggard M, Taylor MW (2014) Influence of environmental variation on symbiotic bacterial communities of two temperate sponges FEMS Microbiol Ecol 88:516–527. doi:10.1111/1574-6941.12317
42. Blanquer A, Uriz MJ, Galand PE (2013) Removing environmental sources of variation to gain insight on symbionts vs. transient microbes in high and low microbial abundance sponges Environ Microbiol 15:3008–3019. doi:10.1111/1462-2920.12261
43. Bright M, Bulgheresi S (2010) A complex journey: transmission of microbial symbionts Nat Rev Microbiol 8:218–230 http://www.nature.com/nrmicro/journal/v8/n3/suppinfo/nrmicro2262_S1.html

44. Reveillaud J, Maignien L, Eren MA, Huber JA, Apprill A, Sogin ML, Vanreusel A (2014) Host-specificity among abundant and rare taxa in the sponge microbiome ISME J 8:1198–1209. doi:10.1038/ismej.2013.227
45. Wiese J, Thiel V, Gärtner A, Schmaljohann R, Imhoff JF (2009) Kiloniella laminariae gen. nov., sp. nov., an alphaproteobacterium from the marine macroalga *Laminaria saccharina* Int J Syst Evol Microbiol 59:350–356. doi:10.1099/ijs.0.001651-0
46. Meron D, Atias E, Iasur Kruh L, Elifantz H, Minz D, Fine M, Banin E (2011) The impact of reduced pH on the microbial community of the coral *Acropora eurystoma* ISME J 5:51–60 http://www.nature.com/ismej/journal/v5/n1/suppinfo/ismej2010102s1.html
47. Becking LE, Renema W, Santodomingo NK, Hoeksema BW, Tuti Y, de Voogd NJ (2011) Recently discovered landlocked basins in Indonesia reveal high habitat diversity in anchialine systems Hydrobiologia 677:89–105. doi:10.1007/s10750-011-0742-0
48. Takai K, Miyazaki M, Hirayama H, Nakagawa S, Querellou J, Godfroy A (2009) Isolation and physiological characterization of two novel, piezophilic, thermophilic chemolithoautotrophs from a deep-sea hydrothermal vent chimney Environ Microbiol 11:1983–1997. doi:10.1111/j.1462-2920.2009.01921.x
49. Urios L, Michotey V, Intertaglia L, Lesongeur F, Lebaron P (2008) Nisaea denitrificans gen. nov., sp. nov. and Nisaea nitritireducens sp. nov., two novel members of the class Alphaproteobacteria from the Mediterranean Sea Int J Syst Evol Microbiol 58:2336–2341. doi:10.1099/ijs.0.64592-0
48. Tapley DW, Buettner GR, Shick JM (1999) Free radicals and chemiluminescence as products of the spontaneous oxidation of sulfide in seawater, and their biological implications Biol Bull 196:52–56
51. Lysek N, Kinscherf R, Claus R, Lindel T (2003) L-5-Hydroxytryptophan: antioxidant and anti-apoptotic principle of the intertidal sponge *Hymeniacidon heliophila* Z Naturforsch C 58:568–572
52. Seeberg E, Eide L, Bjørås M (1995) The base excision repair pathway Trends Biochem Sci 20:391–397. doi:10.1016/S0968-0004(00)89086-6
53. Li G-M (2008) Mechanisms and functions of DNA mismatch repair Cell Res 18:85–98
54. Xie W, Wang F, Guo L, Chen Z, Sievert SM, Meng J, Huang G, Li Y, Yan Q, Wu S, Wang X, Chen S, He G, Xiao X, Xu A (2011) Comparative metagenomics of microbial communities inhabiting deep-sea hydrothermal vent chimneys with contrasting chemistries ISME J 5:414–426 http://www.nature.com/ismej/journal/v5/n3/suppinfo/ismej2010144s1.html
55. Mao Z, Bozzella M, Seluanov A, Gorbunova V (2008) DNA repair by nonhomologous end joining and homologous recombination during cell cycle in human cells Cell Cycle (Georgetown, Tex) 7:2902–2906
56. Morrow KM, Bourne DG, Humphrey C, Botte ES, Laffy P, Zaneveld J, Uthicke S, Fabricius KE, Webster NS (2015) Natural volcanic CO2 seeps reveal future trajectories for host-microbial associations in corals and sponges. ISME J 9:894–908. doi:10.1038/ismej.2014.188